# Calculation of the Vibronic Intensities in the Emission Spectra of Manganese(V) in Oxide Lattices

**David Wexler and Jeffrey I. Zink***

Department of Chemistry and Biochemistry, University of California, Los Angeles, California 90024

*Received April 4, 1994*[⊗]

Vibronic intensities in intraconfigurational spin-forbidden luminescence spectra of Mn(V) in apatite and spodiosite lattices provide a rigorous test for a time-dependent theoretical model. The intensities are induced by spin−orbit coupling between the state corresponding to the spin-forbidden transition and a nearby state corresponding to a spin-allowed transition. Short progressions are observed in totally symmetric Mn−O modes even though no changes in the orbital populations, bond properties, or force constants are expected. The vibronic intensities are calculated by using the numerical integration of the time-dependent Schrödinger equation and the time-dependent theory of electronic spectroscopy. The experimental emission and excitation spectra of Güdel and coauthors provide a rigorous test of the theory because the input parameters are precisely measured or constrained within a narrow range determined by the experimental uncertainty. The calculated intensities of vibronic bands in the emission spectra are in excellent agreement with the measured values. The spectra are interpreted in terms of the probability density of the eigenfunctions of the coupled systems. Trends and sensitivities of the vibronic intensities to changes in the input parameters such as coupling strength, energy separation of the states, and bond length changes between the ground and excited states are discussed.

## Introduction

Intraconfigurational spin-forbidden electronic transitions in transition metal complexes are characterized by a change in the spin multiplicity without any change in the orbital characteristics.[1,2] For example, in tetrahedral $d^2$ complexes, the lowest energy intraconfigurational transition retains the $(e)^2$ orbital configuration. Because no orbital changes are involved in the transition, it might be incorrectly concluded that the electronic spectrum would consist of one line. The simple picture predicts that there would be no bond length changes or force constant changes resulting from the transition and that only the origin ($E_{00}$) band would be observed. However, experimental spectra frequently exhibit small progressions in symmetric normal modes.

A theoretical explanation of the intensities of the components of the vibronic progressions was developed recently.[3,4] The theory is based on the coupling (by spin−orbit coupling) between the state produced by the intraconfigurational transition and a nearby state differing by a spin multiplicity of 1, to which transitions are spin-allowed. The quantum mechanical calculation is not trivial because the coupling of potential surfaces along normal coordinates results in a situation where the Born−Oppenheimer separability of nuclear and electronic wave functions cannot be made.[5]

In a detailed spectroscopic study of Mn(V) ions doped in tetrahedral sites in a variety of oxide lattices, Güdel and coauthors[6−8] measured the intensities of the components of the vibronic progressions in the emission spectra. In addition, they measured the energies of the electronic excited states. The vibrational sideband intensities were then correlated with the singlet/triplet energy separation.[8] They noted that the trends in the vibronic intensities in the spectra of the series of crystals followed the trends in energy separation between the singlet and triplet states as predicted by the theory. These experimental results also provide a rigorous quantitative test of the theoretically calculated intensities because all of the quantities used in the theory are known.

In this paper, the theory of electronic emission spectroscopy from intraconfigurational transitions of tetrahedral $d^2$ metal complexes is described. The theory is applied to the series of experimental emission spectra of Mn(V) ions in apatite and spodiosite lattices. All of the parameters necessary to define the theoretical model are known. These spectra provide a stringent test of the calculations of the intensities of the vibronic components of the emission spectra. The sensitivity of the calculations to the important physical properties of the complexes is discussed, and the intensities are related to excited state properties in the series of crystals.

## Theory

**Physical Picture.** According to the time-dependent theory of electronic emission spectroscopy, the vibrational wave function of the initial electronic state (usually the lowest energy excited state) is multiplied by the electronic transition dipole and placed vertically, according to the Frank−Condon principle, on the final electronic state (usually the ground electronic state). The wave packet is not an eigenfunction of the ground electronic state and therefore begins to evolve. The time dependence of the overlap of the initial wave packet on the time-evolving wave packet (autocorrelation function) determines the width and vibronic structure of the spectrum.[9,10]

[⊗] Abstract published in *Advance ACS Abstracts,* February 15, 1995.

(1) Ballhausen, C. J. *Introduction Ligand Field Theory*; McGraw-Hill: New York, 1962.
(2) Schlaefer, H. L.; Gliemann, G. *Basic Principles of Ligand Field Theory*; Wiley: London, 1969.
(3) Wexler, D.; Zink, J. I.; Reber, C. *J. Phys. Chem.* **1992**, *96*, 8757.
(4) Reber, C.; Zink, J. I. *Comments Inorg. Chem.* **1992**, *13*, 177.
(5) Reber, C.; Zink, J. I. *J. Phys. Chem.* **1992**, *96*, 2681.
(6) Herren, M.; Riedener, T.; Güdel, H. U.; Albrecht, C.; Kaschuba, U.; Reinen, D. *J. Lumin.* **1992**, *53*, 452.
(7) Herren, M.; Güdel, H. U.; Albrecht, C.; Reinen, D. *Chem. Phys. Lett.* **1991**, *183*, 98.
(8) Oetliker, O.; Herren, M.; Güdel, H. U.; Kesper, U.; Albrecht, C.; Reinen, D. *J. Chem. Phys.*, in press.
(9) Heller, E. J. *J. Chem. Phys.* **1975**, *62*, 1544; **1978**, *68*, 3891.
(10) Heller, E. J. *Acc. Chem. Res.* **1981**, *14*, 368.

0020-1669/95/1334-1500$09.00/0 

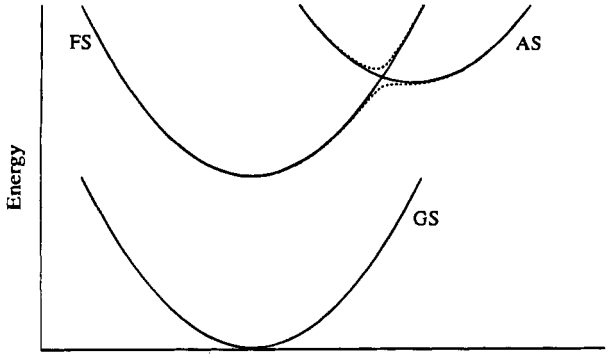


**Figure 1.** Potential energy surfaces for the calculations of the emission spectra of Mn(V) in oxide lattices. The diabatic and adiabatic surfaces are shown as solid and dotted lines, respectively. The highest energy diabatic potential surface AS represents the state to or from which the electronic transition is allowed. The lowest energy diabatic potential surface FS represents the state to or from which the electronic transition is forbidden. This state is undisplaced along the normal coordinate from the ground state GS.

The case where a forbidden electronic transition is made slightly allowed by coupling between two electronic states is more complicated.[3,5] The specific example that is treated here is a spin-forbidden transition that becomes allowed by spin–orbit coupling. A very specific example of potential surfaces corresponding to this situation is shown in Figure 1. In this example, the ground electronic state (GS) is a spin triplet state, the lowest excited state (FS) is a spin singlet, and the next lowest excited state (AS) is again a spin triplet. The minimum of the lowest excited state is at the same position as that of the ground state along the totally symmetric normal coordinate because no orbital change is involved. Emission from the lowest excited state is spin forbidden; emission from the next lowest is spin allowed. Spin–orbit coupling mixes the two states. In this example, the spin–orbit coupling is taken to be a constant along the totally symmetric normal coordinate in the vicinity of the ground electronic state equilibrium internuclear configuration. These diabatic potential energy surfaces form the basis for the model. Coupling between the diabatic surfaces results in an avoided crossing and can be represented by the adiabatic surfaces shown by dotted lines in the figure. Neither of these extremes is entirely correct because coupling of the nuclear and electronic motions is neglected and potential surfaces lose their meaning. In this paper the diabatic basis is chosen as the starting point but the calculations include the coupling of the nuclear and electronic motions (breakdown of the Born–Oppenheimer approximation).

For spin–orbit coupled excited states, shown in Figure 1, the eigenfunction of the lowest vibrational state of the coupled excited state system has two components, one from the lowest energy diabatic potential and the other from the highest energy diabatic potential. In order to keep clear the identity of the diabatic potential surfaces, the lowest energy excited state surface will be called the "forbidden surface, FS" and the highest energy surface the "allowed surface, AS". As selection rules dictate, the components of the wave function are multiplied by their respective transition dipole moments. The transition dipole moment $\mu = 0$ for a forbidden transition and $\mu \neq 0$ for an allowed transition. Therefore, only the component from the AS makes the transition to the ground electronic state. The emission spectrum will show a progression in the ground electronic state frequency because the component of the wave packet from the AS is displaced away from the minimum of the ground state. No progression would be observed if the transition originated purely from the lowest uncoupled surface (assuming that the transition dipole were nonzero) because that surface is not displaced relative to the ground state.

The concept of the eigenfunction of the lowest vibrational level of the coupled excited electronic states being expressed in terms of its projection on the two diabatic potential surfaces is not immediately intuitive. This is true especially when the minimum of one of the diabatic states is much higher in energy than that of the eigenvalue corresponding to the eigenfunction. Further details of the calculations and their physical meanings and examples relevant to the experimental results are presented in the following sections.

The diabatic potential surfaces shown in Figure 1 provide the model for the relevant electronic states of Mn(V) in the oxide lattices ($MnO_4^{3-}$). For the Mn(V) ion in tetrahedral symmetry, the ground state corresponds to $^3A_2$, the FS corresponds to $^1E$, and the AS corresponds to $^3T_2$. The point group of the $MnO_4^{3-}$ ion can be distorted to $C_{3v}$ in the apatite host lattice or to $D_{2d}$ in the spodiosite host lattice. These perturbations of the $T_d$ point group allow the transition to the $^3T_2$ state to become allowed. It is assumed that the nearby $^3T_1$ state (~5000 $cm^{-1}$ higher in energy) does not play a role in the emission process. This assumption is valid because the separation in energy between the $^3T_2$ and $^3T_1$ excited states is on the order of $10^3$ $cm^{-1}$. In the perturbed system, the FS diabatic surface represents the emitting state and the AS diabatic surface is the allowed triplet state to which it is coupled. For crystals with a $D_{2d}$ distortion, the relevant states are $^3B_2$, $^1A_1$, and $^3E$, respectively. For crystals with a $C_{3v}$ distortion, the relevant states are $^3A_2$, $^1E$, and $^3E$, respectively. The normal coordinate is the totally symmetric Mn–O stretch.

**Calculation of Emission.** To calculate the emission spectrum that results from a transition from the ground vibrational state of the coupled excited state system, as in Figure 1, the eigenfunction of the lowest vibrational level must be calculated. This procedure necessitates the calculation of the eigenvalues of the coupled excited states (for example, by calculating the absorption spectrum). The eigenfunction $\Psi_i(E_i)$ corresponding to eigenvalue $E_i$ is calculated by using eq 1,[11–13] where $\phi(t)$ is

$$\Psi_i(E_i) = \int_0^t \phi(t)\, w(t) \exp\left(\frac{iE_i}{\hbar}t\right) dt \qquad (1)$$

the time-dependent (propagating) wavefunction calculated by the method outlined in the Appendix and $w(t)$ is a Hanning window function. The eigenfunction corresponding to the lowest eigenvalue is then multiplied by the transition dipole moment $\mu$ and propagated on the ground state potential surface. For coupled potentials, each eigenfunction $\Psi_i$ is an array with two components corresponding to the projection of the exact eigenstate onto the basis states AS and FS with their respective spins. These projections will be referred to as "the parts of the eigenfunction associated with AS and FS".

The emission spectrum is given by[9,10]

$$I(\omega) = C\omega^3 \int_{-\infty}^{+\infty} \exp(i\omega t)\left\{\langle\phi|\phi(t)\rangle \exp\left(-\Gamma^2 t^2 + \frac{iE_0}{\hbar}t\right)\right\} dt \qquad (2)$$

with $I(\omega)$ the emission intensity at frequency $\omega$, $E_0$ the energy of the electronic origin transition, $\phi$ the initial wave packet (the lowest vibrational level eigenfunction after multiplication by the transition dipole moment), and $\Gamma$ a phenomenological

(11) Feit, M. D.; Fleck, J. A.; Steiger, A. *J. Comput. Phys.* **1982**, *47*, 412.
(12) Kosloff, D.; Kosloff, R. *J. Comput. Phys.* **1983**, *52*, 35.
(13) For an introductory overview see: Tanner, J. J. *J. Chem. Educ.* **1990**, *67*, 917.

**Table 1.**[a] Data Measured from Experimental Spectra

| lattice | spin–orbit coupling: $V_{12}$ | $E_{AS} - E_{FS}$ expt[b] | force constants | | | $^3T_2$ absorption bandwidth: fwhm$_{expt} \times 10^{-3}$ | $R_{10\ expt}$[c] |
|---|---|---|---|---|---|---|---|
| | | | $k_{GS\ expt}$ | $k_{FS\ expt}$ | $k_{AS\ expt}$ | | |
| $Li_3PO_4$ | 120 | 1790 | 800 | 800 | 800 | $2.5 \pm 1$[d] | 0.031 |
| $Sr_5(PO_4)_3Cl$ | 120 | 1450 | 797 | 797 | 797 | $2.0 \pm 0.5$[e] | 0.067 |
| $Ba_5(PO_4)_3Cl$ | 120 | 1320 | 780 | 780 | 780 | $1.0 \pm 0.5$[b] | 0.050 |
| $Ba_5(VO_4)_3Cl$ | 120 | 1210 | 754 | 754 | 754 | $1.0 \pm 0.5$[b] | 0.090 |
| $Ca_2PO_4Cl$ | 120 | 1030 | 788 | 788 | 788 | $2.0 \pm 1$[e] | 0.11 |
| $Sr_2VO_4Cl$ | 120 | 600 | 756 | 756 | 756 | $2.0 \pm 1$[d] | 0.13 |

[a] All numbers in the table are given in wavenumbers ($cm^{-1}$) unless otherwise specified. [b] Güdel, H. U. Private communication. [c] Unitless. [d] Reference 18. [e] Reference 17.

Gaussian damping factor. The most important quantity is $\langle\phi/\phi(t)\rangle$, the autocorrelation function of the initial wave packet $\phi$ prepared on the ground electronic state potential surface after the transition.

The coupling-induced relaxed emission intensity arises from the component of the lowest energy eigenfunction associated with the AS. To calculate the emission spectrum, the component of the eigenfunction from the AS is multiplied by the nonzero transition dipole moment corresponding to the allowed transition from the AS and the component of the eigenfunction from the FS is multiplied by zero, the transition dipole moment for a forbidden transition. Only the component from the AS contributes to the emission intensity. The component from the AS only appears when there is nonzero coupling between the excited state surfaces and vanishes when the coupling is zero.

The input parameters that affect the probability density distribution of the part of the eigenfunction associated with the AS are the coupling strength ($V_{12}$), the energy separation between the minima of the coupled surfaces ($E_{AS} - E_{FS}$), the displacement between the minima of the coupled surfaces ($\Delta$), and the force constants defining the surfaces ($k_{FS}$, $k_{AS}$, $k_{GS}$).[14] As discussed above, the part of the eigenfunction associated with the AS has nonzero probability density only if there is coupling between the AS and the FS.

The dynamics of the wave packet in the time domain provides insight into the emission spectrum in the frequency domain. According to eq 2, the Fourier transform of the autocorrelation function gives the emission spectrum. If the wave packet were not displaced (an eigenfunction of both ground and excited states), the autocorrelation function would be constant in the time domain and therefore transform into an emission spectrum with one sharp spectroscopic feature. When the wave packet is displaced (not an eigenfunction of the ground state surface), it moves away from its initial position, causing $\langle\phi/\phi(t)\rangle$ to decrease. At a later time $T$, corresponding to one vibrational period, the wave packet will return to its initial position, giving rise to a recurrence in the autocorrelation function. The initial decay in the overlap, caused by the movement of $\phi(t)$ along the path of steepest descent, determines the width of the spectrum. The recurrences in the time domain, spaced by time $T$, cause the structure in the frequency domain spaced by $2\pi/T$. The larger the displacement, the steeper the slope, the faster the movement of the wave packet, and the broader the spectrum.

The experimental quantity that provides the rigorous test of the theory is the ratio of the intensity of the first side band ($v = 1$) to that of the emission origin ($v = 0$), $R_{10}$:

$$R_{10} = \frac{\text{emission intensity } (v = 1)}{\text{emission intensity } (v = 0)} \qquad (3)$$

As discussed above, when wave packet displacement is increased, the emission spectra become broader. In broader spectra, vibronic intensity shifts to higher quantum number and hence the ratio $R_{10}$ increases. Therefore by observing trends in the displacement of the part of the eigenfunction associated with AS as a function of input parameter, it is easy to predict the trends in the induced vibronic structure in the emission spectrum and the $R_{10}$ values.

## Comparison of Theory and Experiment

A series of recently published emission spectra of Mn(V) doped into a variety of host lattices containing highly resolved vibronic bands provides a rigorous quantitative test of the theory of vibronic intensity induced by coupling.[6-8] The $R_{10}$ values, given in Table 1, range from 0.03 to 0.13. For an electronic state produced by a purely intraconfigurational transition with no coupling to other states, the $R_{10}$ values should be zero because there is no change in either the force constant or the position of the minimum of the excited state potential surface relative to those of the ground state. The excitation and absorption spectra, together with the emission spectra, provide either exact values of the parameters that define the potential surfaces or else restrict the values to very narrow ranges governed by experimental uncertainty.

The parameters that are needed to define the potential surfaces and thereby calculate the spectra, including the $R_{10}$ values, were outlined in the theory section. These parameters are not variables that can be used to obtain a best fit for the compounds treated here because their values are defined by the highly resolved experimental spectra. The accuracy to which the parameters can be determined fall into three categories: parameters determined directly from the spectra to within a few wavenumbers, parameters defined by the nature of the transitions to within a few wavenumbers, and parameters that are indirectly determined from the spectra with less certainty because of experimental uncertainty.

The parameters that fall into the first category (determined directly from the spectra to within a few wavenumbers) are the force constant of the ground state potential surface ($k_{GS}$), the energy separation between the minima of the coupled surfaces ($E_{AS} - E_{FS}$), the damping factor ($\Gamma$), and the spin–orbit coupling constant ($V_{12}$). The force constants of the ground state potential

(14) For simplicity we choose harmonic potentials in all of the following examples, although the theoretical method is not restricted by the functional form of the potentials. The potentials are given by $V_i(Q) = {}^1/_2\, k_i(Q - \Delta Q_i)^2 + E_i$ with $k_i = 4\pi^2 M(\hbar\omega_i)^2$ the force constant, $\Delta Q_i$ the position of the potential minimum along $Q$, and $E_i$ the energy of the potential minimum for state $i$. The force constants $k_i$, in units of wavenumbers ($cm^{-1}$), are the energies of the fundamentals of the respective potential energy surfaces. These uncoupled potentials are shown as dashed lines in Figure 1 (diabatic potentials). The coupling between the diabatic potentials for states 1 and 2 is chosen to be coordinate independent; i.e., $V_{12} = V_{21} = \text{const}$. Again, the computational method allows us to use coordinate dependent coupling. The most important coupling mechanism in transition metal spectra is spin–orbit coupling which does not strongly depend on nuclear coordinates. For simplicity, we assume a harmonic ground state potential in all examples presented here. The wave functions $\phi_i$ at $t = 0$ are therefore gaussians. Also, for simplicity, the transition moments $\mu_i$ were chosen to be coordinate independent, i.e. constants, in all of the calculations.

**Table 2.** Input Parameters Used in the Calculation of the Emission Intensity Ratio $R_{10}$

| | input $\Delta_{AS}$ for exact match to $R_{10\ expt}$ | | | input $\Delta_{AS}$ corresponding to $fwhm_{expt}$ | | | |
|---|---|---|---|---|---|---|---|
| lattice | $\Delta_{AS}$ (Å) | $10^{-3}fwhm_{AS\ calc}$[b] | $R_{10\ calc}$[d] | $\Delta_{AS}$ (Å) | $10^{-3}fwhm_{AS\ calc}$[b] | $fwhm_{AS\ expt}$[c] | $R_{10\ calc}$[g] |
| $Li_3PO_4$ | 0.053 | 1.60 | 0.031 | 0.095 | 2.5 | $2.5 \pm 1$[d] | 0.069 |
| $Sr_5(PO_4)_3Cl$ | 0.074 | 2.15 | 0.067 | 0.0715 | 2.0 | $2.0 \pm 0.5$[e] | 0.064 |
| $Ba_5(PO_4)_3Cl$ | 0.057 | 1.65 | 0.050 | 0.045 | 1.0 | $1.0 \pm 0.5$[f] | 0.034 |
| $Ba_5(VO_4)_3Cl$ | 0.0845 | 2.256 | 0.090 | 0.045 | 1.0 | $1.0 \pm 0.5$[f] | 0.035 |
| $Ca_2PO_4Cl$ | 0.082 | 2.30 | 0.11 | 0.075 | 2.0 | $2.0 \pm 1$[e] | 0.10 |
| $Sr_2VO_4Cl$ | 0.064 | 1.80 | 0.13 | 0.075 | 2.0 | $2.0 \pm 1$[d] | 0.164 |

[a] The values for the following input parameters were taken directly from Table 1: $V_{12}$, $E_{AS} - E_{FS}$, $k_{GS}$, $k_{FS}$, $k_{AS}$. All numbers in the table are given in wavenumbers ($cm^{-1}$) unless otherwise specified. [b] $Fwhm_{AS\ calc} \propto \omega^2\Delta^2$, where $\omega$ is the force constant of the GS and $\Delta$ is the displacement of the minimum of the AS relative to the GS. [c] Value taken directly from Table 1 for comparison. [d] Reference 18. [e] Reference 17. [f] Güdel, H. U. Private communication. [g] Unitless.

surfaces ($k_{GS}$) were measured directly from the highly resolved emission spectra. The energy difference ($E_{AS} - E_{FS}$) between the origins of the allowed absorption band ($^3T_2$) and the forbidden luminescence band ($^1E$) were measured from experimental excitation spectra.[8] We have used these values for the input values of $E_{AS} - E_{FS}$. In the dibatic basis, $E_{AS}$ and $E_{FS}$ are the measured energies minus the zero-point energies. In the full calculations, including the coupling, the calculated energy separation of the origins of the spectra are within 4 $cm^{-1}$ of the input values for $E_{AS} - E_{FS}$. The phenomenological damping factor ($\Gamma$), which determines the widths of the features in the emission spectrum, was also measured directly from the emission spectra. The coupling parameter used in these calculations is the spin–orbit coupling constant. This value has been determined from EPR and absorption spectroscopic data.[15,16]

The parameters that fall into the second category (those defined by the nature of the transition) are the force constant of the forbidden excited state potential surface ($k_{FS}$) and the displacement of the forbidden excited state potential surface ($\Delta_{FS}$). The force constant of the forbidden excited state $k_{FS}$ is assumed to have the same value as that of the ground state $k_{GS}$. This assumption is based on the fact that the two states only differ by the spin multiplicity. There is no change in orbital population and therefore no change in bond strength. The magnitude of the displacement of the forbidden excited state potential surface along the totally symmetric normal coordinate is zero. This assumption is also based on the absence of change in orbital population.

The parameters that fall into the third category (those indirectly determined from the spectra) are the displacement of the allowed excited state potential surface ($\Delta_{AS}$) and the force constant of the allowed state ($k_{AS}$). The magnitude of the displacement of the allowed excited state potential surface along the totally symmetric normal coordinate can be accurately calculated from the absorption spectrum if vibronic structure corresponding to the mode is resolved. Unfortunately, structure is not resolved in the spectra of any of the compounds treated in this paper. In this paper, a first estimate of $\Delta$ is obtained as described below, and then $\Delta$ is found by fitting the calculated full width at half of the maximum (fwhm) to the experimental fwhm. The magnitude of $\Delta$ is thus calculated from the band widths in the available spectra within narrow error limits determined primarily by the experimental uncertainty. The initial estimate of $\Delta$ is obtained by using eq 4. The experimental

$$\Delta = \{(fwhm)^2/2.773\omega^2\}^{1/2} \quad (4)$$

values of the fwhm for the compounds discussed in this paper contain large experimental uncertainties, given in Table 1.[8,17,18] The experimental uncertainties arise primarily because of overlap with the next higher energy absorption band. Another source of uncertainty is the possible contribution of other normal modes such as a bending mode (vibronic bands corresponding to a bending vibration are observed in the emission spectra). In spite of these sources of uncertainty in $\Delta$, it is constrained by the experimental data to a narrow range of values. The force constant of the allowed excited state can also be measured directly from the absorption spectrum when the band contains vibronic structure. As discussed above, none of the absorption bands considered here contain vibronic structure. The value of $k_{AS}$ will be set equal to the force constant of the ground state ($k_{GS}$). In cases where $k_{AS}$ has been measured for similar changes in orbital population, $k_{AS}$ is 5–10% smaller than $k_{GS}$.[19] Small changes in $k_{AS}$ do not have a large effect on the $R_{10}$ ratios in the emission spectra. The sensitivity of $R_{10}$ to the uncertainties in $\Delta_{AS}$ and $k_{AS}$ is discussed in the next section.

**Calculation of the $R_{10}$ Values.** The calculated $R_{10}$ ratios exactly equal the experimentally measured values when experimental values of the parameters defining the potential surfaces given in the left side of Table 2 are used. The exact numerical agreement between the experimental and calculated $R_{10}$ values is somewhat artificial because a particular value of $\Delta_{AS}$ within the range of experimental uncertainty was chosen. Note however that the values of $\Delta_{AS}$ that are used account for the bandwidth of the allowed band within the uncertainty range. (In other words, if $\Delta_{AS}$ is treated as a fitting variable, exact agreement between the $R_{10}$ values is attained when $\Delta_{AS}$ is in the middle half of its allowed range of variation.) If $\Delta_{AS}$ were fixed at the value required by the best estimate of the bandwidth, the $R_{10}$ values would be in excellent (but not exact) agreement with the experimental ones. The $R_{10}$ values calculated for $\Delta_{AS}$ fixed at the best estimate of the band width are shown in the right side of Table 2. The $R_{10}$ value calculated for the $Ba_5(VO_4)_3Cl$ lattice using the fixed value of $\Delta_{AS}$ has the largest disagreement (a factor of 3). Within the limits of this one-dimensional model and the uncertainty of the $fwhm_{AS\ expt}$, this is an excellent agreement for the ratio.

A sample calculated spectrum is shown in Figure 2. The $R_{10}$ ratio is calculated directly from the $v = 0$ and $v = 1$ peaks in the emission spectrum. The absorption spectrum is calculated by methods described in the Appendix. The fwhm of the absorption spectrum is calculated and given in Table 2.

Because of the excellent agreement between theory and experiment, the model is a good representation of the molecular properties. In the next section, the sensitivity of the $R_{10}$ values

(15) Lachwa, H.; Reinen, D. *Inorg. Chem.* **1989**, *28*, 1044.
(16) Reinen, D.; Lachwa, H.; Allman, R. *Z. Anorg. Allg. Chem.* **1986**, *542*, 71.
(17) Borromei, R.; Oleari, L.; Day, P. *J. Chem. Soc., Faraday Trans.* **1981**, *77*, 1563.
(18) Milstein, J. B.; Ackerman, J.; Holt, S. L. *Inorg. Chem.* **1972**, *6*, 1178.
(19) Hitchman, M. A. *Inorg. Chem.* **1982**, *21*, 821.

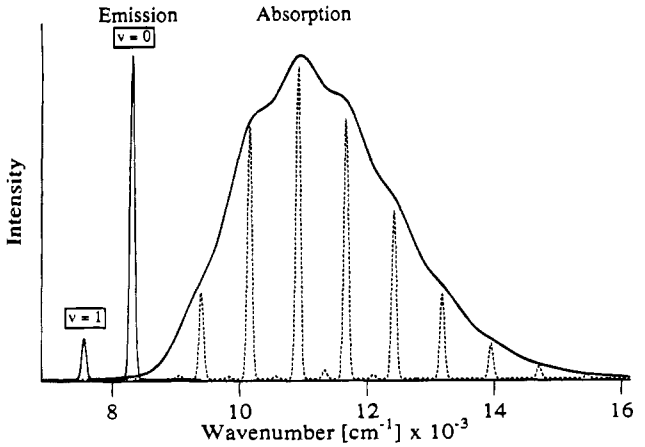


**Figure 2.** Electronic spectra of Mn(V) doped in the $Sr_2VO_4Cl$ lattice as calculated using the input parameters from Table 2. The emission and absorption spectra are shown (normalized to one) with solid lines and are labeled appropriately. The dashed line is the absorption spectrum calculated with a $\Gamma = 25$ cm$^{-1}$ damping factor so that the vibronic structure is resolved.

to changes in the values of the parameters, especially $\Delta_{AS}$, are calculated. In addition, the trends in the emission intensity ($R_{10}$) with changes in the input parameters are interpreted and explained. The trends will be discussed in terms of how the probability density distribution of the part of the eigenfunction from AS is determined from the coupling strength and the shape and position of the coupled excited states.

### Sensitivity and Trends of $R_{10}$

The vibronic structure and intensity are determined by the probability density distribution ("shape") of the part of the eigenfunction from the AS diabatic surface. The shape of the eigenfunction is determined by four main parameters; the magnitude of the coupling constant ($V_{12}$), the energy separation between the minima of the coupled surfaces ($E_{AS} - E_{FS}$), the displacement between the minima of the coupled surfaces ($\Delta$), and the force constants of the coupled surfaces. In this section, the effect of each parameter on the shape of the component of the eigenfunction from the AS is calculated. The trends in the ratio $R_{10}$ are then explained in terms of the trends in the eigenfunction probability density distribution. For the following discussion, the input parameters used in the calculation of the emission spectrum of Mn(V) in the $Sr_5(PO_4)_3Cl$ lattice will provide the starting point from which the trends in $R_{10}$ will be based.

**Coupling Strength.** The part of the eigenfunction associated with the AS for the lowest vibrational level of the coupled excited states displays a trend that is not immediately intuitive. For small values of the coupling constant ($V_{12}$), the eigenfunction associated with the AS has most of its probability near the minimum of the FS. As the coupling between the two excited state potential surfaces increases, the maximum of the probability density moves away from the minimum of the FS toward the minimum of the AS. Eigenfunctions are shown in Figure 3 for two values of $V_{12}$ including zero. As is seen in Figure 3, when the coupling is zero, the eigenfunction is associated entirely with the FS and as $V_{12}$ increases, the probability density associated with the AS increases in magnitude and shifts toward the minimum of the AS.

By knowing the trend in the shape of the part of the eigenfunction associated with the AS, one can predict the trend in $R_{10}$. As the coupling increases, the wave packet has increasing probability away from the minimum of the ground state surface, giving rise to more rapid decreases in $\langle\phi/\phi(t)\rangle$ when

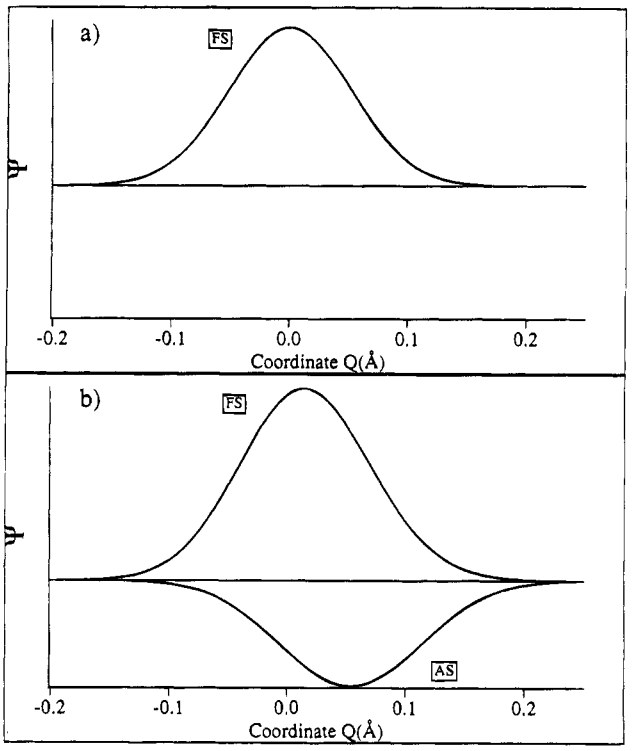


**Figure 3.** Eigenfunctions corresponding to the lowest energy eigenvalue of coupled states of the type illustrated in Figure 1. The sign of the part of the eigenfunction associated with the FS is positive; the sign of the part of the eigenfunction associated with the As is negative. The eigenfunctions are calculated with couplings of (a) 0 cm$^{-1}$ and (b) 1000 cm$^{-1}$.

**Table 3.** Values of the Emission Intensity Ratio ($R_{10}$) with Changes in Input Parameters[a]

| parameter/changed | value of parameter | $R_{10}$ (unitless) |
|---|---|---|
| $E_{AS} - E_{FS}$ (cm$^{-1}$) | | |
| | 1400 | 0.072 |
| | 1500 | 0.067 |
| | 1600 | 0.061 |
| $\Delta_{AS}$ (Å) | | |
| | 0.040: fwhm[b] = 1100 cm$^{-1}$ | 0.025 |
| | 0.074: fwhm = 2100 cm$^{-1}$ | 0.067 |
| | 0.212: fwhm = 5300 cm$^{-1}$ | 0.067 |
| | 0.11: fwhm = 3100 cm$^{-1}$ | 0.096 |
| $k_{AS}$ (cm$^{-1}$) | | |
| | 717 | 0.052 |
| | 797 | 0.067 |
| $V_{12}$ (cm$^{-1}$) | | |
| | 120 | 0.067 |
| | 355 | 0.071 |

[a] All other input parameters are held constant except the parameter listed. [b] Fwhm $\propto \omega^2\Delta^2$, where $\omega$ is the force constant of the GS and $\Delta$ is the displacement of the minimum of the AS relative to the GS.

it is placed on the GS surface and hence to a broader spectrum containing more vibronic features. In a broader spectrum, the vibronic intensity shifts to higher quantum number and the value of $R_{10}$ increases accordingly. The values of $R_{10}$ that result from propagating two eigenfunctions with different $V_{12}$ values on the harmonic ground state surface are given in Table 3. These values of 120 and 355 cm$^{-1}$ were chosen for $V_{12}$ because they are one-quarter and three-quarters of the spin–orbit coupling constant of the Mn(V) free ion. The value of $R_{10}$ increases as the coupling increases, for the reasons discussed above.

The observed trend in the effect of coupling strength on emission intensity discussed above is in agreement with first-order perturbation theory.[20] In the time-dependent calculation, the larger the coupling strength, the greater the emission

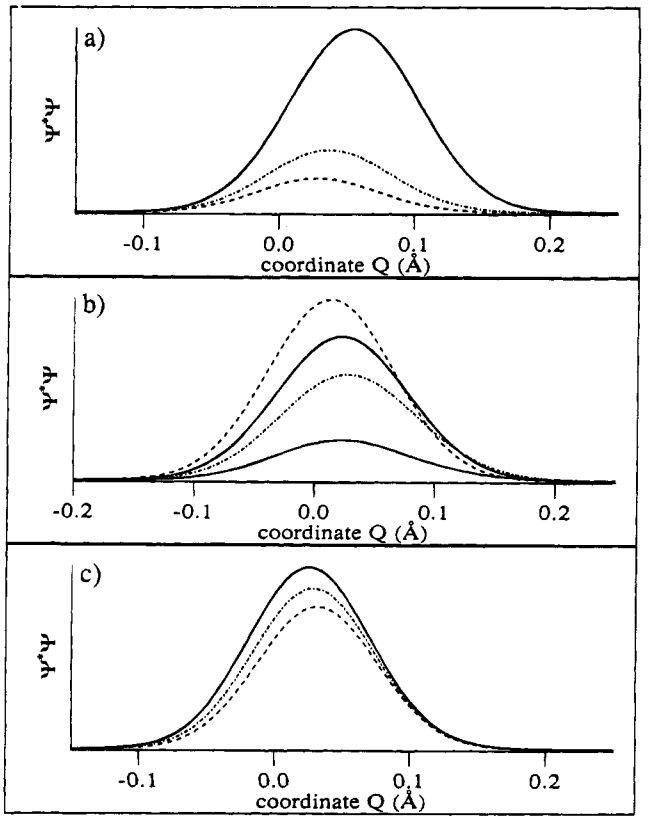


**Figure 4.** Square of the eigenfunctions associated with the AS corresponding to the lowest energy eigenvalue of the coupled states of the type illustrated in Figure 1. (a) The eigenfunctions arising from three values of $E_{AS} - E_{FS}$ are shown: 500 $cm^{-1}$ (solid line), 1000 $cm^{-1}$ (dash–dot line), 1500 $cm^{-1}$ (dashed line). (b) The eigenfunctions are shown for four values of $\Delta_{AS}$. The values of $\Delta_{AS}$ are 0.040 Å (dashed line), 0.076 Å (upper solid line), 0.11 Å (dash–dot line), and 0.21 Å (lower solid line). The two solid lines are the eigenfunctions that give the same value of $R_{10}$ when propagated on the GS. (c) The eigenfunctions arising from three values of $k_{AS}$ are shown: 637 $cm^{-1}$ (solid line); 717 $cm^{-1}$ (dash–dot line); 797 $cm^{-1}$ (dashed line).

intensity.[5] In first-order perturbation theory, the oscillator strength of the forbidden transition ($f_f$) is related to the square of the coupling strength ($H_{spin-orbit}$).

**Energy Separation between Excited States ($E_{AS} - E_{FS}$).** The square of the component of the eigenfunction associated with the AS for the lowest vibrational level of the coupled excited states in Figure 1 is shown for three values of $E_{AS} - E_{FS}$ in Figure 4a. For large values of $E_{AS} - E_{FS}$, the eigenfunction associated with the AS has most of its probability at a position near the minimum of the FS. As $E_{AS} - E_{FS}$ is decreased, the probability moves away from the minimum of the FS toward the minimum of the AS. As the states become closer in energy, the amount of mixing increases and thus the part of the eigenfunction associated with the AS moves toward the minimum of the FS.

As $E_{AS} - E_{FS}$ decreases, the value of $R_{10}$ will increase because the wave packet has increasing probability at a position away from the minimum of the ground state surface. This in turn gives rise to a more rapid decrease in $\langle\phi/\phi(t)\rangle$ and hence to a broader spectrum with intensity at higher quantum numbers. The values of $R_{10}$ that result from propagating the eigenfunctions associated with the AS (nonzero transition dipole moment) on the harmonic ground state potential surface for three different values of $E_{AS} - E_{FS}$ are given in Table 3. The values of 1500 ± 100 $cm^{-1}$ were chosen because they represent upper limits to the magnitude of experimental error in the determination of $E_{AS} - E_{FS}$.

The trend in the probability density of the eigenfunction associated with the AS agrees with first-order perturbation theory.[20] The theory states that the amount of mixing of two spin–orbit coupled states is inversely proportional to the amount of energy separation between those two states ($E_{AS} - E_{FS}$). This trend is seen in the eigenfunctions in Figure 4a. The time-dependent calculation not only agrees with first-order perturbation theory but also explains the vibronic structure.

**Displacement of the Allowed State (AS) along the Normal Coordinate (Δ).** The parts of the eigenfunction associated with the AS for the lowest vibrational level of the coupled excited states are shown for four values of displacement (Δ) of the minimum of the AS along normal coordinate $Q$ in Figure 4b. As the displacement of the AS is increased from zero, the maximum probability of the eigenfunction associated with the AS moves away from the minimum of the FS toward the minimum of the AS. However, as Δ is further increased, the probability density begins to move back toward the FS despite the continued increase of Δ. The value of the normal coordinate $Q$ where the probability reaches a maximum distance from the minimum of the FS will be referred to as $\Delta_c$. Two values of Δ will exist, on either side of $\Delta_c$, that give rise to similar eigenfunctions. The problem of duality can be resolved by using the two values of Δ to attempt to fit the experimental absorption spectrum. By fitting the absorption spectrum and matching the fwhm, the correct value for Δ is found. For example, two $\Delta_{AS}$ values that give the same $R_{10}$ ratio are given in Table 3. Because these $\Delta_{AS}$ values give very different calculated absorption bandwidths, it is easy to choose the one that matches the experimental spectrum. The eigenfunctions for these cases are shown by the solid lines in Figure 4b.

The $R_{10}$ values that correspond to propagation of the above eigenfunctions on the ground state potential surface are shown in Table 3. As Δ increases, the value of $R_{10}$ increases until $\Delta = \Delta_c$, when the value of $R_{10}$ begins to decrease again. As was stated in the previous section, this trend is due to the fact that the wave packet has an increasing probability at a position away from the minimum of the ground state surface with increasing values of $\Delta \leq \Delta_c$.

**Force Constants.** The shape of the eigenfunction associated with the AS for the lowest energy eigenvalue of the coupled excited states is affected by changes in the force constant between the GS and the AS. A typical change in force constant for interconfigurational d–d transitions is −10%.[19] For a decrease of 10% in the force constant (797 to 717 $cm^{-1}$), there is a small but significant change in the $R_{10}$ ratio as shown in Table 3. The parts of the eigenfunction associated with the AS for the lowest energy eigenvalue are shown for three different values of $k_{AS}$ in Figure 4c. Because changes in force constant have an effect on the eigenfunction and therefore the emission spectrum, this trend is presented here. However, for the calculations in this paper, we do not employ any change in force constant.

## Summary

Vibronic structure, characterized by the $R_{10}$ ratio, is induced in the intraconfigurational spin-forbidden luminescence spectra

(20) From first-order perturbation theory, the oscillator strength for the forbidden transition is

$$f_{FS} = f_{AS}\frac{E_{FS}}{E_{AS}}\frac{|\langle\Psi_{AS}|H_{spin-orbit}|\Psi_{FS}\rangle|^2}{(E_{AS} - E_{FS})^2}$$

where $E_{FS}$ and $E_{AS}$ are the energies of the forbidden and allowed electronic transitions, $H_{spin-orbit}$ is the coupling between AS and FS, and $\Psi_{AS}$, $\Psi_{FS}$ are the wave functions associated with the AS and FS, respectively.

of Mn(V) ions in oxide lattices. The structure is caused by spin–orbit coupling of the undisplaced singlet state with a displaced triplet state. The spectra are calculated on the basis of a model containing two excited state potential surfaces and one vibrational coordinate (the totally symmetric Mn–O stretch). An exact quantum mechanical calculation based on numerical integration of the time-dependent Schrödinger equation that includes coupling of the nuclear and electronic motions (breakdown of the Born–Oppenheimer approximation) is used. The lowest energy eigenfunction of the coupled excited states has two components, the most important one corresponding to the projection on the allowed triplet diabatic surface. The probability density of this component is shifted away from the minimum of the ground state surface, and propagation of this component on the ground state surface leads to nonzero $R_{10}$ values. Increasing the coupling strength, decreasing the energy separation between the singlet and triplet states, increasing the displacement of the triplet state (up to a limit), and increasing the force constant of the triplet state all cause an increase in the $R_{10}$ ratio because of an increase in the distance of the maximum of the probability density away from the minimum of the ground state surface. The parameters used in the theory to define the diabatic potential surfaces are obtained from the experimental spectra. These spectra, from eight different lattices, provide a rigorous test of the theory.

**Acknowledgment.** This work was made possible by a grant from the National Science foundation (CHE 9106471). We thank Prof. H. Güdel for giving us the excitation data before they were published and for valuable discussions regarding the Mn(V)-doped lattices.

## Appendix: Calculation of Absorption Spectra

According to the time-dependent theory of electronic spectroscopy, the absorption spectrum $I(\omega)$ is given by[9,10]

$$I(\omega) = C\omega \int_{-\infty}^{+\infty} \exp(i\omega t) \left\{ \langle \phi | \phi(t) \rangle \exp\left( -\Gamma^2 t^2 + \frac{iE_0}{\hbar} t \right) \right\} dt \qquad \text{(A1)}$$

where all of the quantities are the same as those in eq 2.

The spectrum is governed by the dynamics of the wave packet on excited state potential surfaces. The wave packets $\phi(t)$ evolve on these surfaces with time. For absorption transitions to two coupled excited states, two wave packets, $\phi_1$ and $\phi_2$, moving on the two coupled potential surfaces are needed.[5,21–27] The propagating wave functions, $\phi_i(t)$, are given by the time-dependent Schrödinger equation. For two coupled states it is given by[11]

$$i\frac{\partial \phi_i}{\partial t} = \begin{pmatrix} H_1 & V_{12} \\ V_{21} & H_2 \end{pmatrix} \begin{pmatrix} \phi_1 \\ \phi_2 \end{pmatrix} \qquad \text{(A2)}$$

where $H_i$ denotes the Hamiltonian, $V_i(Q)$ is the potential energy as a function of the configurational coordinate $Q$, and $-{}^1/_2\mathrm{M}\cdot\nabla^2$ is the nuclear kinetic energy.

The split operator method developed by Feit and Fleck is used to calculate $\phi_i(t)$.[11–13] Both the configurational coordinate $Q$ and the time are represented by a grid with points separated by $\Delta Q$ and $\Delta t$, respectively. For one surface, the time-dependent wave function $\phi(Q,t+\Delta t)$ is obtained from $\phi(Q,t)$ with

$$\phi(t+\Delta t) = \exp\left( \left( \frac{i\Delta t}{4M} \right) \nabla^2 \right) \exp(-i(\Delta t)V) \exp\left( \left( \frac{i\Delta t}{4M} \right) \nabla^2 \right) \phi(Q,t) + O[(\Delta t)^3] = \hat{P}\hat{V}\hat{P}\,\phi(Q,t) + O[(\Delta t)^3] \qquad \text{(A3)}$$

The generalization of this equation to the case of two coupled potentials requires that the exponential operators $\hat{P}$ and $\hat{V}$ in eq A3 be replaced by $2 \times 2$ matrices operating simultaneously on $\phi_1(Q,t)$ and $\phi_2(Q,t)$

$$\begin{pmatrix} \phi_1(Q,t+\Delta t) \\ \phi_2(Q,t+\Delta t) \end{pmatrix} = \begin{pmatrix} \hat{P}_1 & 0 \\ 0 & \hat{P}_2 \end{pmatrix} \begin{pmatrix} \hat{V}_1 & \hat{V}_{12} \\ \hat{V}_{21} & \hat{V}_2 \end{pmatrix} \begin{pmatrix} \hat{P}_1 & 0 \\ 0 & \hat{P}_2 \end{pmatrix} \begin{pmatrix} \phi_1(Q,t) \\ \phi_2(Q,t) \end{pmatrix} + O[(\Delta t)^3] \qquad \text{(A4)}$$

The kinetic energy operator $\hat{P}$ is independent for $\phi_1$ and $\phi_2$ in the diabatic basis; i.e., its matrix is diagonal. The potential energy operator $\hat{V}$ is more intricate. The exponential operators must be given in terms of potentials that diagonalize the potential matrix in the total Hamiltonian, eq A4, i.e. in terms of the adiabatic potentials $V_a$ and $V_b$. These potentials are calculated from the diabatic potentials $V_1$ and $V_2$ and the coupling $V_{12}$:

$$V_a = c_1 V_1 + c_2 V_2 = {}^1/_2\{(V_1 + V_2) - \sqrt{(V_1 - V_2)^2 + 4V_{12}}\} \qquad \text{(A5)}$$

$$V_b = c_2 V_1 - c_1 V_2 = {}^1/_2\{(V_1 + V_2) + \sqrt{(V_1 - V_2)^2 + 4V_{12}}\} \qquad \text{(A6)}$$

From eq A4 it is obvious that $\phi_1(t)$ and $\phi_2(t)$ are mixed (formally via the off-diagonal matrix elements $\hat{V}_{12}$) at each time step. Details of the computer implementation of eq A4 are given in the literature.[5,21–27]

Amplitude transfer between surfaces due to coupling causes a forbidden transition to gain intensity in the absorption spectrum. A forbidden transition means that the initial wave packet to that state is multiplied by zero (the transition dipole moment) and therefore has no amplitude on that particular excited electronic state. However, for the allowed transition, the wave packet is multiplied by the nonzero transition dipole moment and the wave packet is transferred vertically from the ground state onto the AS potential surface. When coupling between the two states is nonzero, amplitude transfer occurs between the AS and FS. The greater the amplitude transfer to the FS, the greater the intensity of the transition to that state in the absorption spectrum.

IC940355H

(21) Reber, C.; Zink, J. I. *J. Phys. Chem.* **1992**, *96*, 571.
(22) Alvarellos, J.; Metiu, H. *J. Chem. Phys.* **1988**, *88*, 4957.
(23) Jiang, X. P.; Heather, R.; Metiu, H. *J. Chem. Phys.* **1989**, *90*, 2555.
(24) Heather, R.; Metiu, H. *J. Chem. Phys.* **1989**, *90*, 6903.
(25) Zhang, J.; Heller, E. J.; Huber, D.; Imre, D. G.; Tannor, D. *J. Chem. Phys.* **1988**, *89*, 3602.
(26) Das, S.; Tannor, D. *J. Chem. Phys.* **1989**, *91*, 2324.
(27) Zhang, J.; Heller, E. J.; Huber, D.; Imre, D. G. *J. Phys. Chem.* **1991**, *95*, 6129.